Carbohydrate Polymers 82 (2010) 189–194

Contents lists available at ScienceDirect

Carbohydrate Polymers

journal homepage: www.elsevier.com/locate/carbpol

Novel chitosan/gold-MPA nanocomposite for sequence-specific oligonucleotide detection

Shunsheng Cao[a], Rajeev Mishra[b], Srikanth Pilla[c], Swapnil Tripathi[d], Manoj K. Pandey[e], Gopit Shah[f], Ajay K. Mishra[g], Mani Prabaharan[h], Shivani B. Mishra[g], Jin Xin[a], R.R. Pandey[i], Weiwei Wu[a], Avinash C. Pandey[j], Ashutosh Tiwari[a,*]

[a] School of Materials Science and Engineering, Jiangsu University, Zhenjiang 212 013, China
[b] Department of Cancer Genetics, School of Medicine, Nihon University, Tokyo 173 8610, Japan
[c] Department of Civil & Environmental Engineering, Stanford University, Stanford, CA 94305, USA
[d] Department of Physics & Astronomy, University of Wisconsin-Barron County, Barron County, WI, USA
[e] Department of Frontier Materials, Graduate School of Engineering, Nagoya Institute of Technology, Gokiso-cho, Showa-ku, Nagoya-shi 466 8555, Japan
[f] Department of Biological Sciences, University of Wisconsin-Milwaukee, Milwaukee, WI 53211, USA
[g] Department of Chemical Technology, University of Johannesburg, Doornfontein, Johannesburg 17011, South Africa
[h] Department of Chemistry, Faculty of Engineering and Technology, SRM University, Kattankulathur 603 203, India
[i] Division of Engineering Materials, National Physical Laboratory, New Delhi 110 012, India
[j] Nano Phosphor Application Centre, University of Allahabad, Allahabad 211 002, India

ARTICLE INFO

Article history:
Received 3 March 2010
Received in revised form 16 April 2010
Accepted 21 April 2010
Available online 29 April 2010

Keywords:
DNA biosensor
Sequence-specific detection
Chitosan
Thiol caped gold NPs
Nanocomposite electrode

ABSTRACT

A 20-mer single-stranded oligodeoxyribonucleotide (ssODNs) was covalently probed onto the nanocomposite electrode, made up of an indium-tin oxide (ITO) glass surface coated with chitosan (CHIT), which is bonded with carboxyl functionalized thiol capped gold nanoparticles (gold-mercaptopropionic acid, Au-MPA NPs). The prepared CHIT/Au-MPA/ITO and the ssODNs/CHIT/Au-MPA/ITO electrodes were characterized with FTIR spectroscopy, scanning electron microscopy (SEM), transmission electron microscopy (TEM) and cyclic voltammetry (CV). TEM micrograph of the composite electrode showed that Au-MPA NPs had the diameter ranging from 4 to 16 nm. The ssODNs/CHIT/Au-MPA/ITO electrode showed a linear increase in the amperometric current with an increasing concentration of the single-stranded target complementary ODNs (cODNs) within the range of 0.03–325 fM. The ssODNs/CHIT/Au-MPA/ITO electrode exhibited a sensitivity of 0.572 μA/fM with a response time of 12 s. The ssODNs/CHIT/Au-MPA/ITO electrode had a shelf life of ~182 days, when stored at 4 °C.

1. Introduction

The DNA sequencing is a promising technique to determine the precise sequence of nucleotides in a DNA sample. The sequencing technique has advantage in many research areas including comparative genomics and evolution, forensics, epidemiology, and applied medicine for diagnostics and therapeutics (Tilley, Marcelli, Wilson, & McPhaul 1989). The change in DNA sequence causes various genomic diseases. Detection of such changes occurred on the DNA chain is an important strategy for biomedical diagnostics (Fackenthal & Olopade, 2007; Tiwari & Gong, 2009; Uygun, 2009). The current technology viz. micro array and real time polymerase chain reaction (RT-PCR) has disadvantages of being indirect, expensive, laborious and short on selectivity (Qin, Yung, & Yue, 2007). Thus there is an essential need for the development of new methods for sensitive, stable and cost effective detection of sequence-specific oligonucleotides.

In the recent years, electrochemical nucleic acid biosensors have received much attention due to their rapid response, high sensitivity, and inherent selectivity (Mousty, 2010; Ron & Rishpon, 2010; Shan et al., 2010; Wei et al., 2009). The electrochemical detection technique provides a simple, accurate, and inexpensive platform for molecular detection. The performance of such biosensor generally depends on the physico-chemical properties of the electrode materials, as well as the sensing element immobilized over the electrode surface. Most of the reported electrochemical biosensors usually apply a high positive charge potential on the working electrode, which minimizes the interference effects from the reducing species (Cao et al., 2009; Wang, Huang, Shan, Foley, & Tao, 2010; Wang, Yang, & Jiao, 2009).

Meanwhile, chitosan (CHIT) is a moderately inexpensive and stable electroactive material that allows for mass-production of biosensors. It is one of the most widely used biopolymers for sensor applications due to its nontoxic nature, excellent film

* Corresponding author. Tel.: +86 511 8879 0191; fax: +86 511 8879 0769.
E-mail address: ashunpl@gmail.com (A. Tiwari).

0144-8617/$ – see front matter © 2010 Elsevier Ltd. All rights reserved.
doi:10.1016/j.carbpol.2010.04.051

forming ability, good mechanical strength, high permeability, and cost-effectiveness (Kerman, Saito, & Tamiya, 2008; Li, Liu, Liu, Liu, & Yao, 2005; Tiwari & Gong, 2008; Tiwari & Singh, 2007). CHIT is a non-conducting biomaterial; however, it has an excellent biocompatible property that favours the immobilization of biomolecules over its surface (Kerman et al., 2008). The surface shielding of sensing element, i.e., the complementary oligodeoxyribonucleotide (cODNs) or single-stranded oligodeoxyribonucleotide (ssODNs), is one of the key challenges for fabricating a highly sensitive DNA biosensor (Abbaspour & Mehrgardi, 2004; Tlili, Youssoufi, Ponsonnet, Martelet, & Renault, 2005). It was reported that modifying CHIT with metals and metal oxides such as gold improves its redox properties which influence the electron-transfer kinetics during the course of electrochemical detection (Li et al., 2005).

Moreover, gold nanoparticles (NPs) permit direct electron transfer between redox biological moieties and bulk electrode materials, which allows electrochemical sensing to be performed without the need for electron-transfer mediators. Various characteristics of gold NPs, such as their high surface-to-volume ratio, their high surface energy, their ability to decrease the distance between proteins and metal particles, and their ability to act as an electron-conducting pathway between prosthetic groups and the electrode surface, may facilitate electron transfer between redox biological moieties and the electrode surface (Thaxton, Georganopoulou, & Mirkin, 2006; Zhao, Brook, & Li, 2008). Hence, gold NPs have been shown to provide useful interfaces at which redox processes of molecules involved in biochemical reactions of analytical significance can be electrocatalyzed (Ofir, Samanta, & Rotello, 2008).

The size and surface morphology are important parameters when applying the NPs for biosensing that can be controlled or modified experimentally through functionality as well as with adjusting the preparation conditions. In this study, chitosan/gold-mercaptopropionic acid/indium-tin oxide (CHIT/Au-MPA/ITO) has been investigated as a promising sensing electrode for sequence-specific ssODNs. Specifically a 20-mer ssODNs probe was covalently immobilized onto the surface of a CHIT/Au-MPA/ITO electrode and with this electrode; the complementary pair of probed ssODNs, i.e., cODNs was electrochemically detected by a change in current with respect to concentration. The advantageous features of present biosensor include a low price, ease of preparation, high sensitivity, and good selectivity.

2. Experimental methods

2.1. Materials

CHIT (Sigma–Aldrich, >85% deacetylated), 3-mercaptopropionic acid (Aldrich, 99%), sodium borohydride (Aldrich, 99%), hydrogen tetrachloroaurate (III) hydrate (Aldrich, 99.99%), 1-ethyl-3-(3-dimethylaminopropyl) carbodiimide hydrochloride (EDC, Aldrich, 99%) and *N*-hydroxysuccinimide (NHS, Aldrich, 99%) were used without further purification. All solutions were prepared with 18.2 MΩ deionized water. Indium-tin-oxide (ITO) coated glass (Balzers) sheets with a resistance of 15 Ω/cm were used as substrates for the deposition of electrodes. The sequence of primers was purchased from Sigma–Aldrich and used for the detection of oligonucleotide. The following sequences of the primers were employed for this study:

Probe ssODNs: 5′-GGACGTAAATCCTATCGGTC-3′
Target cODNs: 5′-CCTGCATTTAGGATAGCCAG-3′
Mismatch ssODNs: 5′-GGACGTATATCCTATCGGTC-3′

To prepare the CHIT solution, 1.0 g of CHIT flakes was dissolved into 100 mL of 1.0% acetic acid solution. The resulting mixture was stirred for 3 h at room temperature until the CHIT flakes were completely dissolved. The CHIT solution was stored in a refrigerator at 4 °C until further use.

2.2. Synthesis of thiol caped gold (Au-MPA) NPs

To prepare the thiol caped gold (i.e., Au-MPA) NPs, concentrated solutions of tetrachloroauric acid ($HAuCl_4$) and 3-mercaptopropionic acid (MPA) were first prepared in ethanolic acetic acid (0.001 M). Thereafter, 10 mL of a solution containing 6 mM $HAuCl_4$ and 12 mM MPA was prepared by diluting the concentrated stock solutions with ethanol. All solutions were prepared fresh prior to reduction. Reduction was carried out by adding 65 μL of a 1.4 M aqueous solution of sodium borohydride ($NaBH_4$) in 5 μL portions under constant stirring. To form stable thiol monolayers on the gold NPs, the suspension was allowed to stir slowly overnight in a dark at room temperature for 24 h. After that, the Au-MPA NPs suspension was placed into an eppendorf tube and washed three times (centrifugation at 5000 rpm for 30 min) with ethanol to remove excess alkanethiol from the suspension.

2.3. Self-assembling of Au-MPA NPs onto CHIT (CHIT/Au-MPA)

Au-MPA NPs were covalently attached onto CHIT backbone using EDC and NHS as the condensing agents at room temperature (Fig. 1c). In a typical experiment, 50 mg of Au-MPA NPs was dissolved in 10 mL DMSO and activated with 0.3 mM of EDC and NHS at room temperature. Next, 15 mL of 1% CHIT was added to the solution and the resulting solution mixture was stirred for 24 h. After that, the solution mixture was filtered to remove the insoluble by-products, residual impurities, and aggregates. The final product was recovered by precipitation with cold diethylether and dried under vacuum.

2.4. Fabrication of CHIT/Au-MPA/ITO electrode

CHIT/Au-MPA (50 mg) was dispersed in 15 mL chloroform and mechanically agitated for 24 h. 10 μL of the resulting CHIT/Au-MPA solution was uniformly spread on the ITO substrate by spin coating technique and dried at room temperature (Fig. 1a). The CHIT/Au-MPA/ITO electrode was washed with deionized water followed by a phosphate buffer saline (PBS) solution (pH 7.0) in order to neutralize the electrode surface.

2.5. Immobilization of ssODNs probe onto CHIT/Au-MPA/ITO electrode

The ssODNs probed bioactive electrode was prepared by covalent immobilization of the ssODNs over the CHIT/Au-MPA/ITO electrode. The CHIT/Au-MPA/ITO electrode was immersed in phosphate buffer solution (0.1 M, pH 7.0) containing 0.03 M EDC and 0.03 M NHS for 2 h, then immediately pipetted out 15 μL of ssODNs (5 mM) over the electrode surface and kept at room temperature for 5 h. The resulting ssODNs probed CHIT/Au-MPA/ITO bioelectrode was thoroughly washed with water and rinsed with a PBS of pH 7.0 to rinse off any loosely bound ssODNs from the electrode (Fig. 1b).

2.6. Hybridization of cODNs onto CHIT/Au-MPA/ITO electrode

The hybridization reaction was carried out by pipetting 15 μL of buffer containing 10 mM Tris–HCl, 1.0 mM EDTA, and 0.10 M NaCl on the surface of the electrode, which holds with different molar concentration of the cODNs ranging from 0.03 to 325 fM. The resulting electrode was kept at 42 °C for 50 min, and then washed

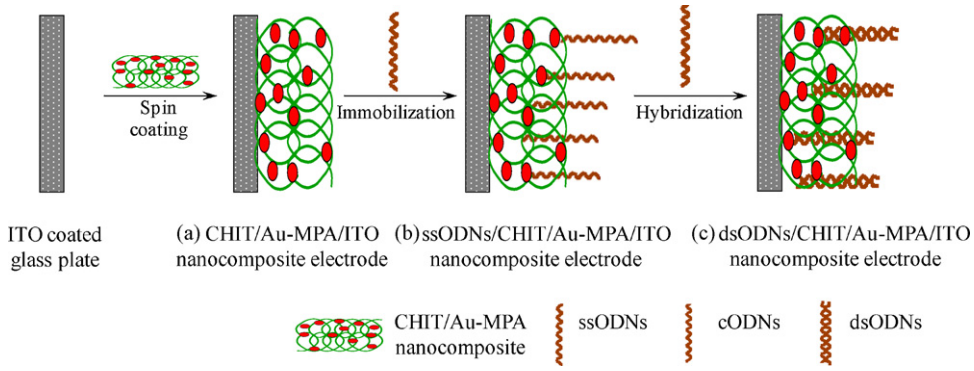

Fig. 1. Schematic presentation of the (a) preparation of CHIT/Au-MPA/ITO electrode; (b) ssODNs/CHIT/Au-MPA/ITO electrode; and (c) hybridization of the cODNs onto ssODNs/CHIT/Au-MPA/ITO electrode.

with PBS of pH 7.0 to remove the unhybridized cODNs over the CHIT/Au-MPA/ITO electrode. A similar procedure was adopted for the mismatched ssODNs (Fig. 1c).

2.7. Characterizations

FTIR spectra were recorded on a PerkinElmer – BX II spectrophotometer. The surface topology of the electrodes was studied using SEM (JEOL-840) operated at 15 kV. The electrodes were sputter-coated with a thin layer of gold (~20 nm) prior to the morphological examination. TEM was carried out with dispersed CHIT/Au-MPA composite matrix on 400 mesh carbon coated copper grid using FEI-Morgagni-268D TEM.

Electrochemical measurements of the electrodes were performed with a Potentiostat/Glavanostat (Princeton Applied Research, 273 A) unit with three electrodes in PBS of pH 7.0. The working electrode was one of the following three electrodes fabricated: CHIT/Au-MPA/ITO; ssODNs/CHIT/Au-MPA/ITO; and target cODNs hybridized CHIT/Au-MPA/ITO. Platinum foil and Ag/AgCl were used as the counter and reference electrode, respectively. The electrochemical detection was performed in 50 mM PBS of pH 7.0 containing 5 mM $Fe(CN)_6^{3-/4-}$ at 30 mV s^{-1} scan rate. All measurements were carried out at 25 °C.

3. Results and discussion

3.1. Electrodes fabrication and characterizations

The thiol caped gold NPs (Au-MPA) were synthesized by reacting $HAuCl_4$ with 3-mercaptopropionic acid (i.e., acid functionalized alkane thiol precursor) followed by $NaBH_4$ reduction (Mandal, Fleming, & Walt, 2002) as shown in Fig. 2a. Thereafter, CHIT macromer was mechanically agitated with Au-MPA NPs. Within the resultant CHIT/Au-MPA nanocomposite, the Au-MPA NPs covalently self assembled onto the CHIT backbone through the –CO–NH– bonds as revealed in Fig. 2b.

The CHIT/Au-MPA nanocomposite with free –COOH and $–NH_2$ groups were covalently bonded ssODNs over the composite

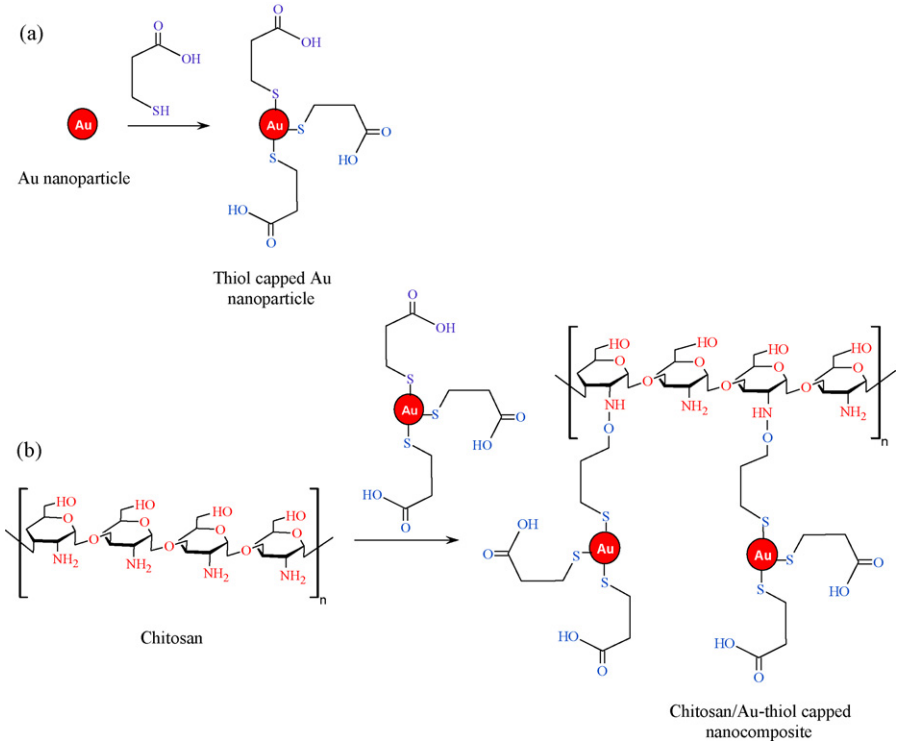

Fig. 2. (a) Synthesis of thiol capped gold (Au-MPA) NPs and (b) Alignment of Au-MPA NPs within the CHIT backbone via the intermolecular hydrogen bonding.

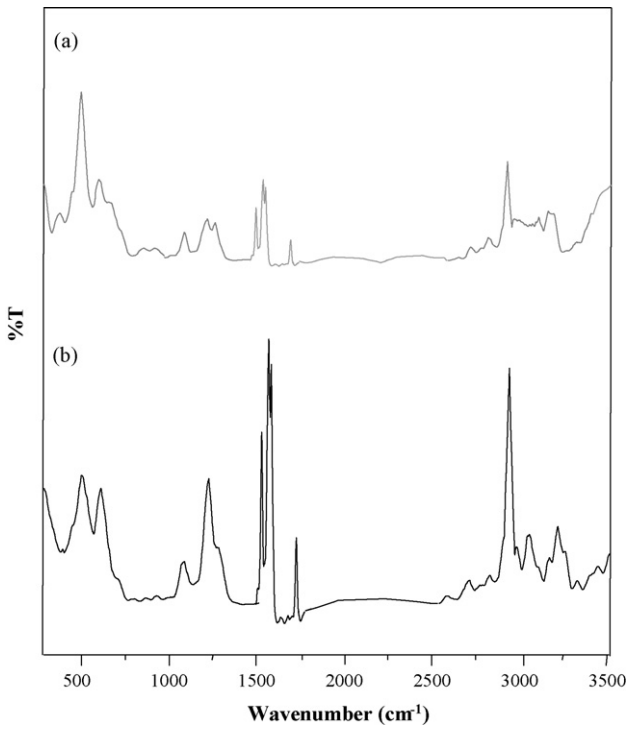

Fig. 3. FTIR spectra of the (a) CHIT/Au-MPA/ITO, and (b) ssODNs/CHIT/Au-MPA/ITO electrodes.

electrode surface through the amide linkages using NHS and EDC as the coupling agents during the bioelectrode preparation process (Xu, Cai, He, & Fang, 2001). Fig. 1 shows the overall steps for fabrication of the CHIT/Au-MPA/ITO and ssODNs/CHIT/Au-MPA/ITO electrodes.

The FTIR spectrum of the CHIT/Au-MPA/ITO electrode (Fig. 3a) illustrated the characteristic peaks of Au-MPA, as well as CHIT. The following key characteristic bands were observed: (1) 3170–3380 cm^{-1} (O–H and N–H stretching); (2) 2800–2950 cm^{-1} (C–H stretching of alkane thiol chain); (3) 2650–2780 cm^{-1} (S–H stretching); (4) 1728 cm^{-1} (C=O stretching of free –COOH groups); (5) 1621 cm^{-1} (–CO–NH– stretching, a typical absorption appeared due to covalent attachment of CHIT's $–NH_2$ group and Au-MPA's –COOH group); and (6) 500–900 cm^{-1} (Au–S vibrations).

The FTIR spectrum of the ssODNs/CHIT/Au-MPA/ITO electrode (Fig. 3b) showed phosphate vibration at 1244 cm^{-1} (accredited from phosphate backbone of immobilized ssODNs) with the peaks broadening at (1) 3140–3410 cm^{-1} (addition of N–H stretching vibration); (2) 2810–2960 cm^{-1}; (3) 1738 cm^{-1} (C=O stretching); and (4) 1636 cm^{-1} due to the attachment of ssODNs with the CHIT/Au-MPA matrix. Hence, FTIR spectra confirmed the immobilization of ssODNs onto the CHIT/Au-MPA/ITO electrode.

The surface morphology of the electrodes was observed with SEM as shown in Fig. 4a and b. Both electrodes exhibited a relatively rough regular surface topology, which may facilitate the immobilization of ssODNs in the case of the CHIT/Au-MPA/ITO electrode. The TEM micrograph (Fig. 4c) of the CHIT/Au-MPA/ITO electrode exhibited Au-MPA NPs with the diameter ranging from 4 to 16 nm. The particle-size distribution curve (Fig. 4d) was obtained from the TEM image analysis of the CHIT/Au-MPA/ITO electrode. It was observed that about 70% of Au-MPA NPs in the CHIT/Au-MPA/ITO electrode were found within the diameter ranging from 6 to 10 nm. This reveals that Au-MPA NPs were homogeneously distributed in the CHIT/Au-MPA/ITO electrode with a control size range.

3.2. Electrochemical measurements

Fig. 5 shows the electrochemical characteristics of bare, ssODNs immobilized, and ODNs hybridized CHIT/Au-MPA/ITO electrodes. The CHIT/Au-MPA/ITO electrode illustrated admirable electrochemical performance (Fig. 5a). It was observed that the CHIT/Au-MPA/ITO electrodes could carry out the electrochemical response of $Fe(CN)_6^{3-/4-}$, which is attributed the excellent electronic behaviour of Au-MPA NPs and the strong ability of CHIT to interact with the redox $Fe(CN)_6^{3-/4-}$ ions due to the presence of $–NH_2$ groups (Tang, Su, Tang, Ren, & Chen, 2010). Among the three types of electrodes investigated, the peak current of the dsODNs/CHIT/Au-MPA/ITO electrode was the highest while that of the CHIT/Au-MPA/ITO electrode was the lowest. The increase in the peak current observed with the ssODNs/CHIT/Au-MPA/ITO electrode (Fig. 5b) was attributed to the prompt redox behaviour of ssODNs (Zhang, Wang, Gong, & He, 2005). Further increase in the peak current measured with the cODNs hybridized ssODNs/CHIT/Au-MPA/ITO electrode (Fig. 5c) to ssODNs/CHIT/Au-MPA/ITO electrode may be due to formation of dsODNs zwitterion surface on the ssODNs/CHIT/Au-MPA/ITO electrode (Zhang, Chen, Chen, Chen, & Fu, 2009).

The rate of hybridization of target cODNs to the ssODNs can be described mathematically using a variation of Freundlich equation

$$x \equiv \frac{h}{c} = KM^{\varepsilon} \tag{1}$$

where h is the concentration of hybridized cODNs and c is the total concentration of probed ssODNs on the working electrode, M is the molar concentration of the target cODNs in the solution, and x is the ratio of hybridized cODNs to the total number of probe ssODNs. Here, K and ε are empirical constants. Taking a logarithm we get

$$\log(x) = \log(K) + \varepsilon \log(M) \tag{2}$$

As peak oxidation current for ssODNs/CHIT/Au-MPA/ITO electrode is lower than the cODNs hybridized ssODNs/CHIT/Au-MPA/ITO electrode at 0.4 V. The ssODNs/CHIT/Au-MPA/ITO electrode, which is partially hybridized with target cODNs can be modelled as a part of electrical circuit with resistors connected in parallel. Let G_p is the conductance of the ssODNs/CHIT/Au-MPA/ITO electrode and G_h is the conductance of cODNs hybridized ssODNs/CHIT/Au-MPA/ITO electrode. Conductance is reciprocal of resistance.

$$G = \frac{1}{R} \quad \text{and} \quad I = GV \tag{3}$$

here R is the resistance, I is the current and V is the applied voltage.

Then the conductance of the cODNs hybridized ssODNs/CHIT/Au-MPA/ITO electrode can be written as

$$G = xG_h + (1-x)G_p = (G_p - x(G_p - G_h)) \tag{4}$$

By combining all the above equations current's dependence on M (molar concentration of target cODNs available for hybridization with ssODNs over the ssODNs/CHIT/Au-MPA/ITO electrode surface) can be written as

$$I = V(A - B\log M) \tag{5}$$

where A and B are positive constants which depend on (G_p, G_h, K and ε).

Eq. (5) potentially explains the current dependence as a function of molar concentration of target cODNs. The ssODNs hybridization biosensor typically shows a linear increasing in the current with increasing concentration of the target cODNs. The equation further supports the linear current dependence with the logarithm of molar concentration of target cODNs available for hybridization with immobilized ssODNs of the ssODNs/CHIT/Au-MPA/ITO electrode.

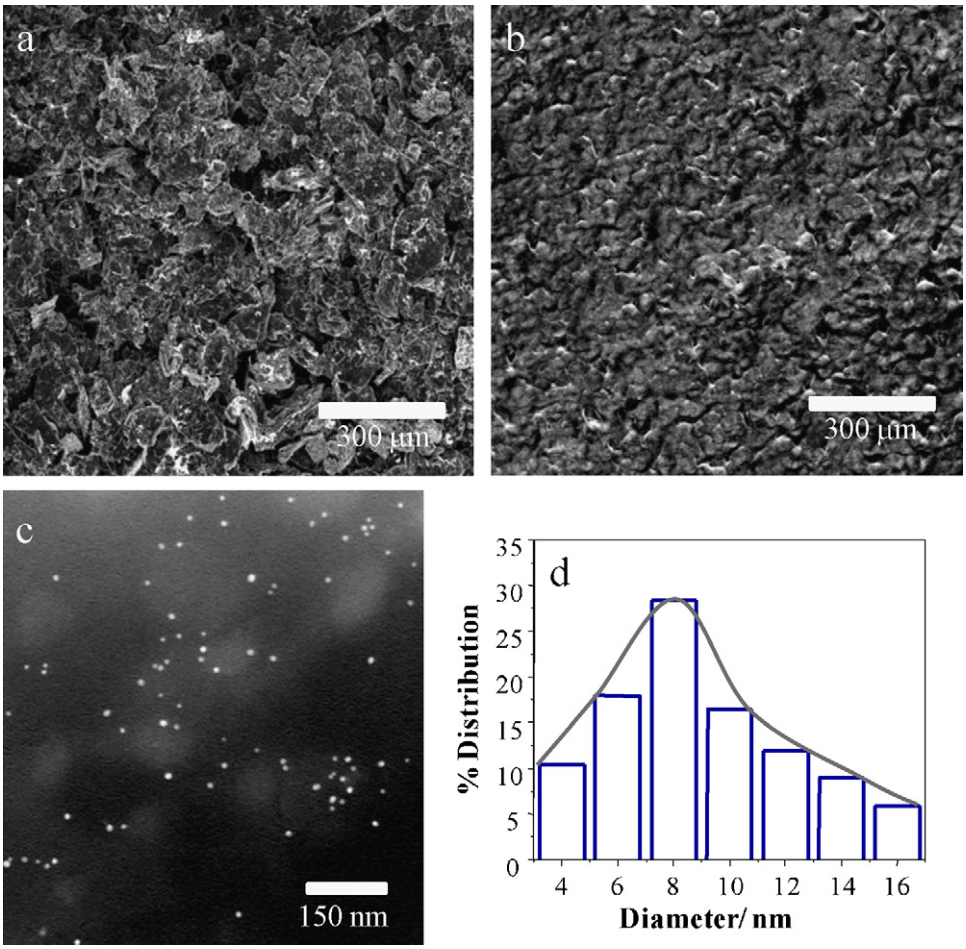

Fig. 4. SEM micrographs of the (a) CHIT/Au-MPA/ITO, and (b) ssODNs/CHIT/Au-MPA/ITO electrodes; (c) TEM image of CHIT/Au-MPA/ITO electrode; and (d) particle-size distribution of Au-MPA NPs in CHIT/Au-MPA/ITO electrode.

Fig. 6 shows the calibration curve of the peak current measured with CV using the ssODNs/CHIT/Au-MPA/ITO electrode at varying molar concentrations of the cODNs ranging from 0.03 to 325 fM. It was found that the peak oxidation current observed at about 0.4 V decreased with an increasing concentration of the target cODNs until 325 fM, beyond which the peak oxidation current remained as a constant. In fact, as shown in Eq. (5), the peak oxidation current decreased linearly with an increasing logarithm of cODNs molar concentration. This result indicates that binding ssODNs with

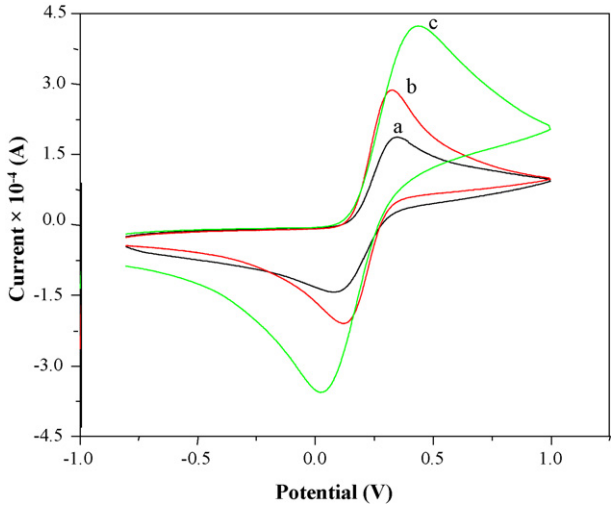

Fig. 5. Cyclic voltammograms of the (a) CHIT/Au-MPA/ITO; (b) ssODNs/CHIT/Au-MPA/ITO; and (c) dsODNs/CHIT/Au-MPA/ITO electrodes in PBS (50 mM, pH 7.0, and 5 mM $Fe(CN)_6^{3-/4-}$) at 30 mV s^{-1} scan rate.

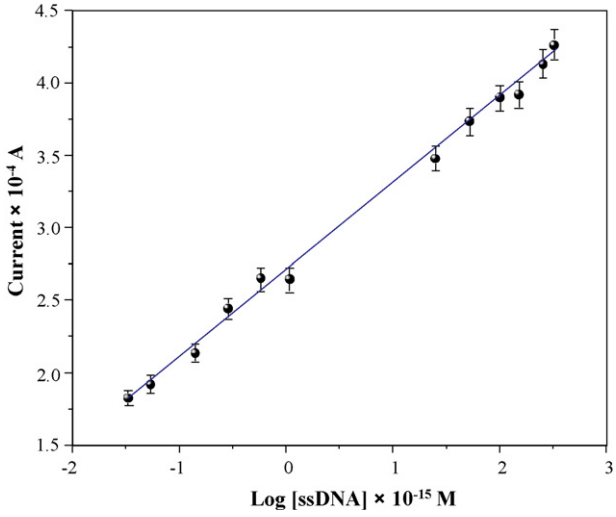

Fig. 6. Steady-state current dependence calibration curve of the ssODNs/CHIT/Au-MPA/ITO bioelectrode with respect to logarithm of cODNs molar concentration; working conditions: PBS 50 mM of pH 7.0, and 5 mM $Fe(CN)_6^{3-/4-}$ at potential 0.4 V vs. Ag/AgCl.

the cODNs at the ssODNs/CHIT/Au-MPA/ITO electrode surface had occurred. Moreover, it shows that 325 fM of cODNs is sufficient to saturate the ssODNs immobilized CHIT/Au-MPA/ITO electrode surface, and 0.03 fM was detection limit of the biosensor. The sensitivity of the ssODNs/CHIT/Au-MPA/ITO bioelectrode measured was 0.572 μA/fM and it responded in 12 s. In addition, the surface concentration of the ionic species on the ssODNs/CHIT/Au-MPA/ITO was 4.906 mM/cm^2, calculated by measuring the oxidation current of CV at different scan rates.

3.3. Reproducibility and accuracy

The lowest detection limit of the ssODNs/CHIT/Au-MPA/ITO electrode was 0.03 fM. The reproducibility of the response of the bioelectrode was investigated at a 50 fM target cODNs concentration. No significant decrease in current response was observed after at least 10 uses in testing; thus, the bioelectrode displayed a good reproducibility. The relative standard deviation was found to be about 6% determined by five successive measurements of a 50 fM target cODNs standard using a single biosensor with the same ssODNs/CHIT/Au-MPA/ITO electrode. In a series of ten biosensors using ten different ssODNs/CHIT/Au-MPA/ITO electrodes, a relative standard deviation of about 4% was obtained for the individual current response of the same sample (50 fM target cODNs). The good reproducibility observed with the biosensor may be attributed to the efficient bonding of the ssODNs with the CHIT/Au-MPA nanocomposite matrix.

3.4. Thermal stability and shelf life

The thermal stability of the ssODNs/CHIT/Au-MPA/ITO electrode was studied by measuring the current at different temperatures ranging from 4 to 45 °C in the presence of 50 fM target cODNs. It was observed that the ODNs hybridization rate increased with the temperature up to 32 °C and the optimum temperature range was between 29 and 32 °C due to the increased kinetic energy of the ODNs. The storage stability of the ssODNs/CHIT/Au-MPA/ITO electrode was amperometrically measured and a similar current response was found after storing for 182 days at 4 °C.

3.5. Interference study

The selectivity of the biosensor was investigated by the hybridization of the ssODNs immobilized CHIT/Au-MPA/ITO bioelectrode with one-base-mismatch cODNs sequences. After incubation with the mismatched cODNs sequence, the bioelectrode showed a negligible decrease in the peak oxidation current at 0.4 V, indicating that the biosensor had good selectivity only for the target cODNs.

The reproducibility of the biosensor was measured with a 25 fM cODNs sequence. The response current with five ssODNs/CHIT/Au-MPA/ITO electrodes fabricated under similar conditions had an average current response of 2.36×10^{-4} A with a standard deviation of ±0.02. Thus, the biosensor showed excellent reproducibility.

4. Conclusion

A 20-mer ssODNs was covalently immobilized onto the CHIT/Au-MPA/ITO electrode. The obtained ssODNs/CHIT/Au-MPA/ITO bioelectrode was applied for the detection of cODNs and exhibited an excellent sensitivity and reproducibility. The voltammetric sensitivity of the biosensor was found at 0.572 μA/fM with a detection limit of 0.03 fM. The specificity of the biosensor was monitored via one-base mismatched ssODNs. The amperometric response of the ssODNs/CHIT/Au-MPA/ITO bioelectrode for the cODNs was barely affected with the mismatched ssODNs. Current efforts aim to develop a novel bioelectrode using Au NPs/carbohydrate polymer, CHIT based material for the efficient and precise detection of complementary ODNs associated with polygenic disease viz. cancer.

References

Abbaspour, A., & Mehrgardi, M. A. (2004). Electrocatalytic oxidation of guanine and DNA on a carbon paste electrode modified by cobalt hexacyanoferrate films. *Analytical Chemistry*, *76*, 5690–5696.

Cao, Q., Zhao, H., Zeng, L., Wang, J., Wang, R., Qiu, X., et al. (2009). Electrochemical determination of melamine using oligonucleotides modified gold electrodes. *Talanta*, *80*, 484–488.

Fackenthal, J. D., & Olopade, O. I. (2007). Breast cancer risk associated with *BRCA1* and *BRCA2* in diverse populations. *Nature Reviews Cancer*, *7*, 937–948.

Kerman, K., Saito, M., & Tamiya, E. (2008). Electroactive chitosan NPs for the detection of single-nucleotide polymorphisms using peptide nucleic acids. *Analytical Bioanalytical Chemistry*, *391*, 2759–2767.

Li, J., Liu, Q., Liu, Y., Liu, S., & Yao, S. (2005). DNA biosensor based on chitosan film doped with carbon nanotubes. *Analytical Biochemistry*, *346*, 107–114.

Mandal, T. K., Fleming, M. S., & Walt, D. R. (2002). Preparation of polymer coated gold NPs by surface-confined living radical polymerization at ambient temperature. *Nano Letters*, *2*, 3–7.

Mousty, C. (2010). Biosensing applications of clay-modified electrodes, a review. *Analytical Bioanalytical Chemistry*, *396*, 315–325.

Ofir, Y., Samanta, B., & Rotello, V. M. (2008). Polymer and biopolymer mediated self-assembly of gold NPs. *Chemical Society Review*, *37*, 1814–1825.

Qin, W. J., Yung, L., & Yue, L. (2007). Nanoparticle-based detection and quantification of DNA with single nucleotide polymorphism (SNP) discrimination selectivity. *Nucleic Acid Research*, *35*, 1–8.

Ron, E. Z., & Rishpon, J. (2010). Electrochemical cell-based sensors. *Advanced Biochemistry Engineering Biotechnology*, doi:10.1007/10-2009-17

Shan, C., Yang, H., Han, D., Zhang, Q., Ivaska, A., & Niu, L. (2010). Electrochemical determination of NADH and ethanol based on ionic liquid-functionalized graphene. *Biosensor Bioelectronics*, *25*, 1504–1508.

Tang, D., Su, B., Tang, J., Ren, J., & Chen, G. (2010). Nanoparticle-based sandwich electrochemical immunoassay for carbohydrate antigen 125 with signal enhancement using enzyme-coated nanometer-sized enzyme-doped silica beads. *Analytical Chemistry*, *82*, 1527–1534.

Thaxton, C. S., Georganopoulou, D. G., & Mirkin, C. A. (2006). Gold nanoparticle probes for the detection of nucleic acid targets. *Clinical Chemistry Acta*, *363*, 120–126.

Tilley, W. D., Marcelli, M., Wilson, J. D., & McPhaul, M. J. (1989). Characterization and expression of a cDNA encoding the human androgen receptor. *Proceedings of National Academy of Sciences of the United States of America*, *86*, 327–331.

Tiwari, A., & Gong, S. (2009). Electrochemical detection of a breast cancer susceptible gene using cDNA immobilized chitosan-*co*-polyaniline electrode. *Talanta*, *77*, 1217–1222.

Tiwari, A., & Gong, S. (2008). Electrochemical study of chitosan-SiO_2-MWNT composite electrodes for the fabrication of cholesterol biosensors. *Electroanalyst*, *20*, 2119–2126.

Tiwari, A., & Singh, V. (2007). Synthesis and characterization of electrical conducting chitosan-*graft*-polyaniline. *Express Polymer Letters*, *1*, 308–317.

Tlili, C., Youssoufi, H. K., Ponsonnet, L., Martelet, C., & Renault, N. J. J. (2005). Electrochemical impedance probing of DNA hybridisation on oligonucleotide-functionalised polypyrrole. *Talanta*, *68*, 131–137.

Uygun, A. (2009). DNA hybridization electrochemical biosensor using a functionalized polythiophene. *Talanta*, *79*, 194–198.

Wang, S., Huang, X., Shan, X., Foley, K. J., & Tao, N. (2010). Electrochemical surface plasmon resonance, basic formalism and experimental validation. *Analytical Chemistry*, *82*, 935–941.

Wang, X., Yang, T., & Jiao, K. (2009). Electrochemical sensing the DNA damage in situ induced by a cathodic process based on Fe@Fe(2)O(3) core-shell nanonecklace and Au NPs mimicking metal toxicity pathways *in vivo*. *Biosensor Bioelectronics*, *25*, 668–673.

Wei, F., Patel, P., Liao, W., Chaudhry, K., Zhang, L., Arellano-Garcia, M., et al. (2009). Electrochemical sensor for multiplex biomarkers detection. *Clinical Cancer Research*, *15*, 4446–4452.

Xu, C., Cai, H., He, P., & Fang, Y. (2001). Electrochemical detection of sequence-specific DNA using a DNA probe labeled with aminoferrocene and chitosan modified electrode immobilized with ssDNA. *Analyst*, *126*, 62–65.

Zhang, J., Chen, J. H., Chen, R. C., Chen, G. N., & Fu, F. F. (2009). Sequence-specific detection of trace DNA via a junction-probe electrochemical sensor employed template-enhanced hybridization strategy. *Biosensor Bioelectronics*, *25*, 815–819.

Zhang, R. Y., Wang, X. M., Gong, S. J., & He, N. Y. (2005). Electrochemical detection of single a-g mismatch using biosensing surface based on gold NPs. *Genomics Proteomics Bioinformatics*, *3*, 47–51.

Zhao, W., Brook, M. A., & Li, Y. (2008). Design of gold nanoparticle-based colorimetric biosensing assays. *ChemBioChem*, *9*, 2363–2371.